Ray tracing channel simulation for millimeter wave indoor localization system

Research thesis

Zheming Yin

Institute of Signal Processing and System Theory

University of Stuttgart

18.07.2024

Motivation

- Millimeter wave indoor localization system based on active radar sensing of local passive reference points [1]

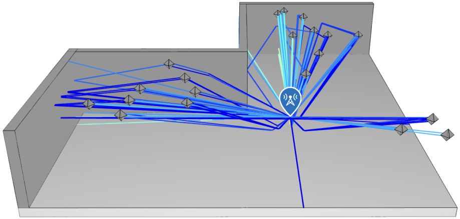

Figure 0.1. The conceptual view of the millimeter wave indoor localization system

- Ray tracing channel simulation
- Large and realistic environment

Motivation

- Frequency-modulated continuous wave (FMCW) radar

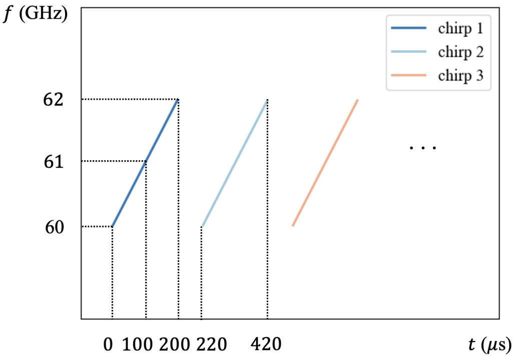

Figure 0.2. The principle of the FMCW radar

Goal

- The signal flow

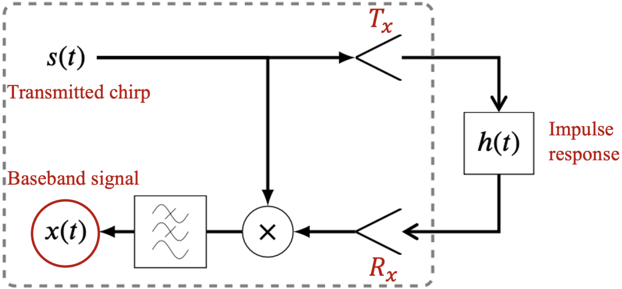

Figure 0.3. The view of the signal flow [2]

- Range-Doppler (RD) map and constant false alarm rate (CFAR) detection

Table of Contents

Table of Contents

Blender

- Modeling of the reflectors

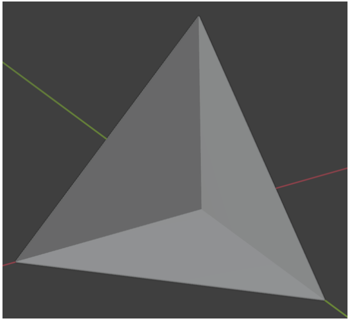

Figure 1.1. Trihedral corner reflector

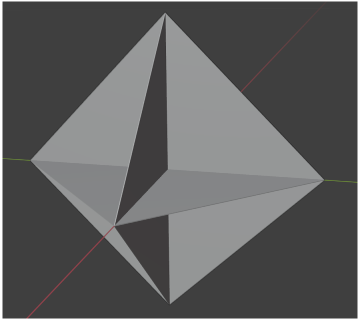

Figure 1.2. Octahedral reflector

Blender

- Modeling of the room model

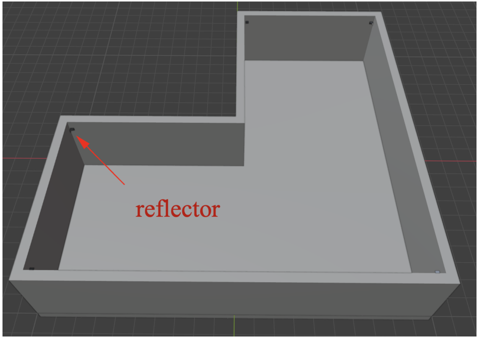

Figure 1.3. Room model with reflectors

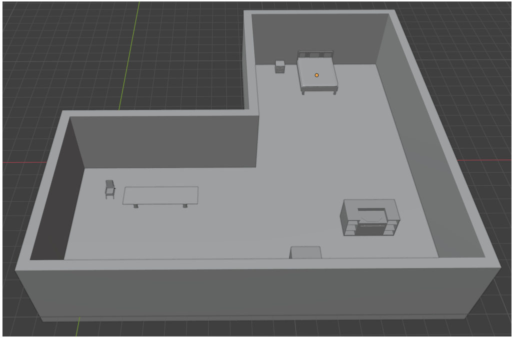

Figure 1.4. Room model with furniture [3]

Raytracer

- Setup of the raytracing (MaxNumreflections, MaxAbsolutePathLoss, Method, etc.)
- The shooting and bouncing ray (SBR) method

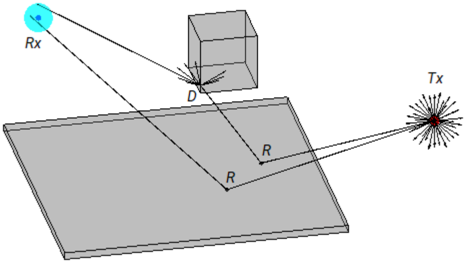

Figure 1.5. The view of the SBR method [4]

Raytracing

- The view of raytracing in the empty room model and room model with furniture

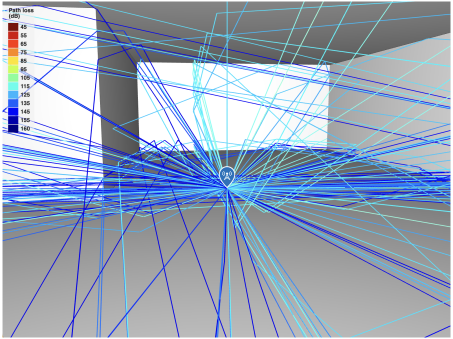

Figure 1.6. In empty room model

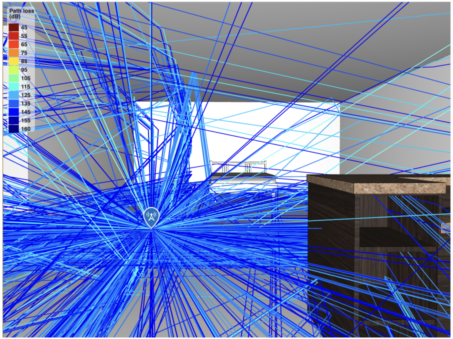

Figure 1.7. In room with furniture

Raytracer

- The view of raytracing in the room model with reflectors and inside the reflector

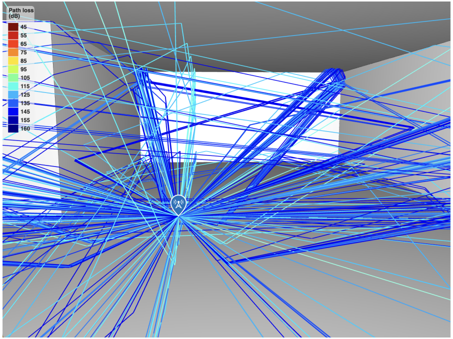

Figure 1.8. In room with reflectors

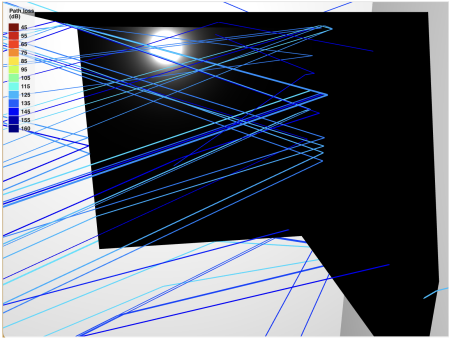

Figure 1.9. The view inside the reflector

Line-of-sight (LOS) rays

- Setting the receivers at the positions of reflectors to obtain LOS rays

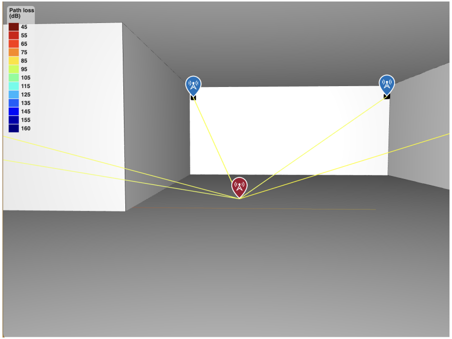

Figure 1.10. LOS rays from five trihedral corner reflectors

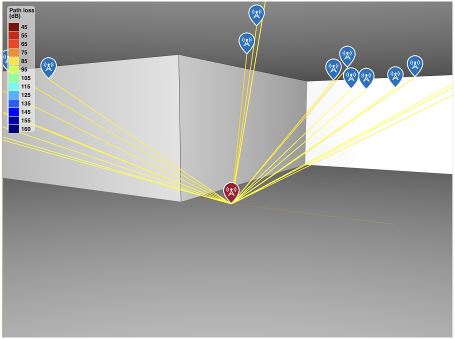

Figure 1.11. LOS rays from multiple octahedral reflectors

Path loss (PL)

$$PL = 10 \cdot \log_{10}\left(\frac{G_T G_R \lambda^2 \cdot \sigma}{(4\pi)^3 r^4}\right) [5], \tag{1}$$

where

- G_T and G_R are the gain values of transmitter and receiver respectively.
- λ is the wavelength of the ray.
- σ is the radar cross section.
- r represents the propagation distance of LOS rays.

The signal model

$$x(n_s, n_p) = \sum_m A_m \exp\left(2\pi j \left(\frac{2Br_m}{T_c c} T_s n_s + \frac{2fv_m}{c} T_p n_p\right)\right) + n(n_s, n_p)\ [6], \qquad (2)$$

where

- $x(n_s, n_p)$ is an element of a 2D matrix $\mathbf{X}$, i.e. baseband signal,
- n_s = 1...256 is the fast time samples,
- n_p=1...32 is the slow time samples,
- m represents each ray in the channel simulation,
- $A_m = \sqrt{P_T \cdot 10^{-PL_m/10} \cdot R}$,
- the first term for the delay and the second term for the Doppler effect,
- $n(n_s, n_p)$ is the Gaussian noise $n \sim \mathcal{CN}(0, V_{noise})$.

Range-Doppler map

- The view of 2D fast Fourier transform (FFT) and range-Doppler map

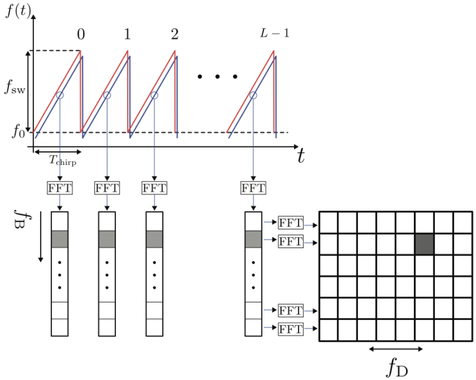

Figure 1.12. The view of 2D FFT [7]

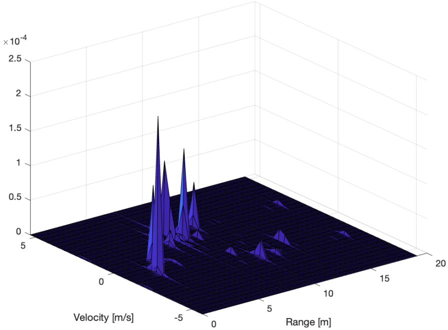

Figure 1.13. Range-Doppler map

Constant false alarm rate (CFAR) detection

- The CFAR plots for the empty room model and room model with reflectors

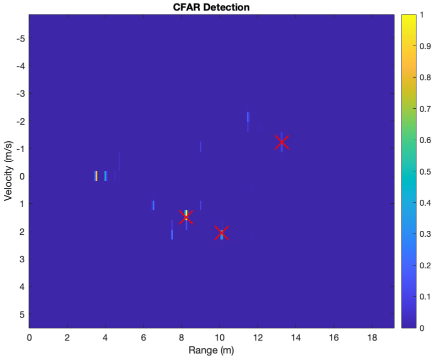

Figure 1.14. In the empty room

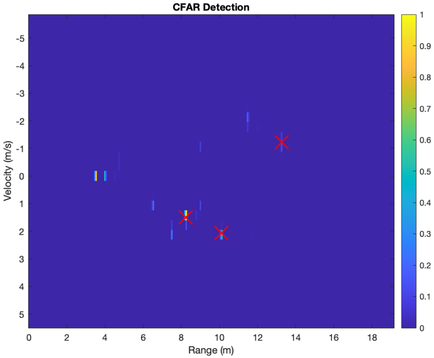

Figure 1.15. In the room with reflectors

Constant false alarm rate (CFAR) detection

- The CFAR plots for the room model with reflectors and with furniture

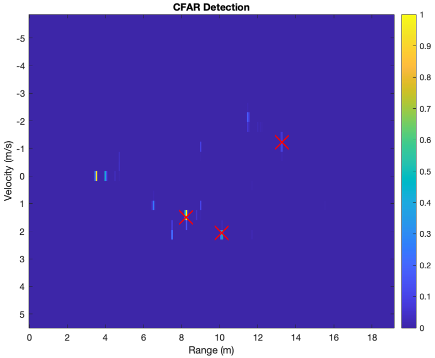

Figure 1.16. In the room with reflectors

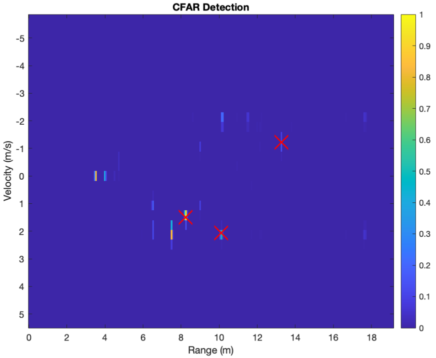

Figure 1.17. In the room with furniture

Table of Contents

Antenna designer

- "Optimization" function to obtain maximum gain value

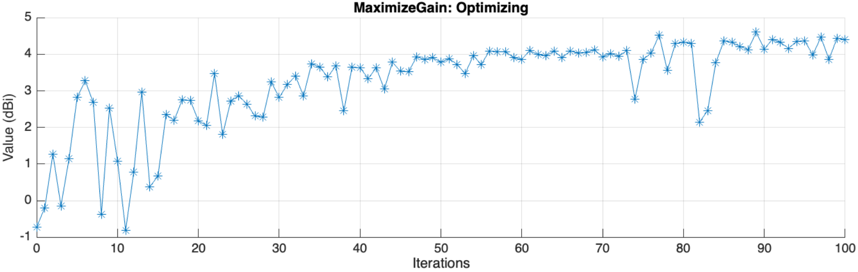

Figure 2.1. The view of the maximum gain

Antenna designer

- The gain as $az = 0^{\circ}$ between the first version and after tuning

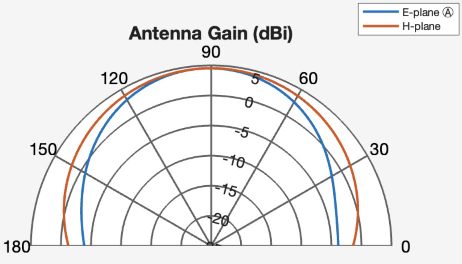

Figure 2.2. The gain of the first version

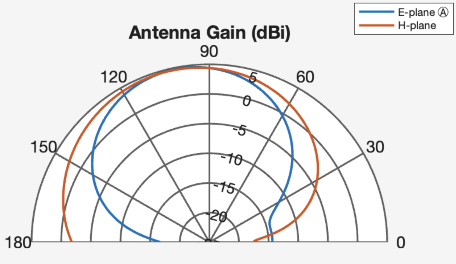

Figure 2.3. The gain after tuning

Antenna designer

- The view and radiation pattern of the final antenna

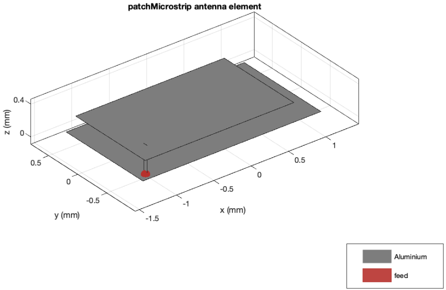

Figure 2.4. View of the final antenna

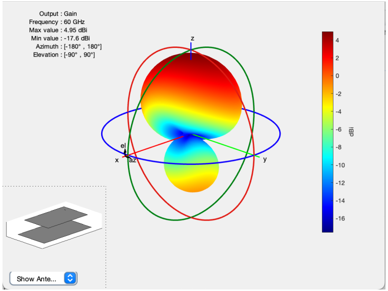

Figure 2.5. 3D radiation pattern

- The constant false alarm rate (CFAR) plots about the radiation pattern

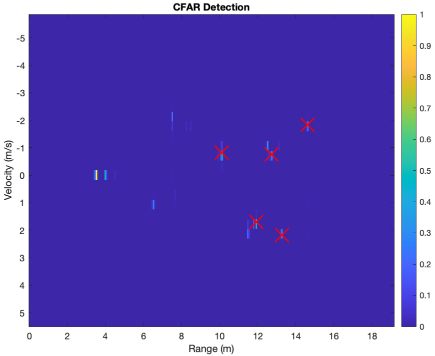

Figure 2.6. CFAR without radiation pattern

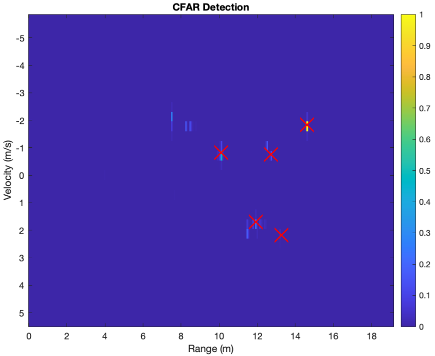

Figure 2.7. CFAR with radiation pattern

Results

- The view of the asymmetric radiation pattern in the room

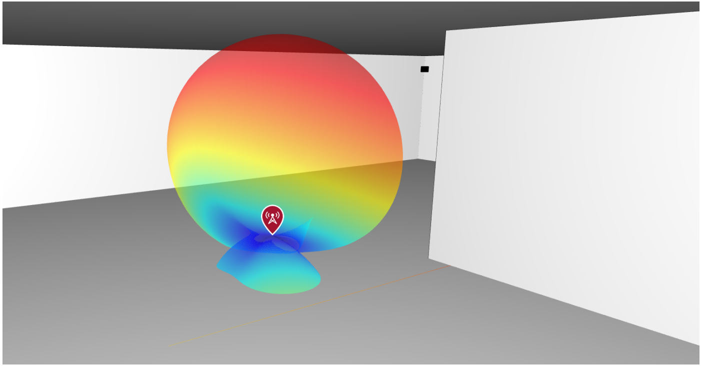

Figure 2.8. The view of the asymmetric pattern

Table of Contents

Radar cross section (RCS)

- View of the RCS for the tetrahedral object with default parameters

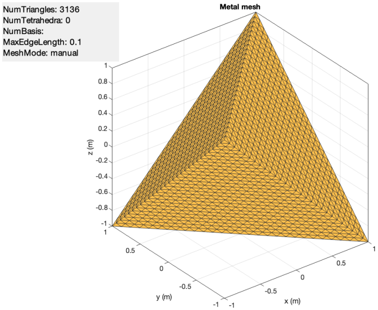

Figure 3.1. Mesh of the tetrahedral object

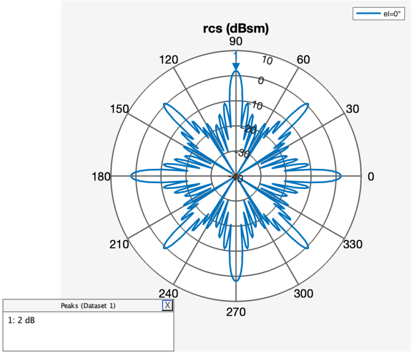

Figure 3.2. 2D RCS of the tetrahedral object

Radar cross section (RCS)

- View of the RCS for the tetrahedral object with scaled parameters

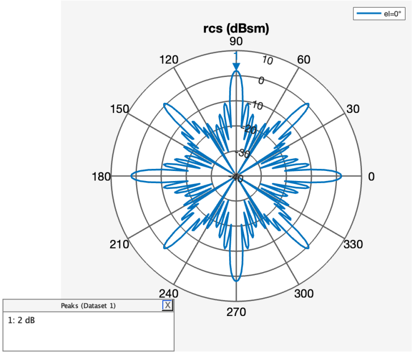

Figure 3.3. 2D RCS without scaling

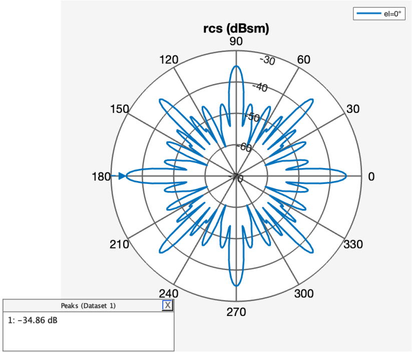

Figure 3.4. 2D RCS with scaling

Radar cross section (RCS)

- View of the RCS for the trihedral corner reflector

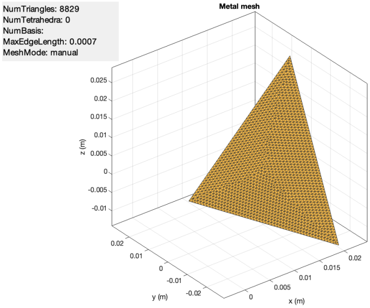

Figure 3.5. Mesh of trihedral corner reflector

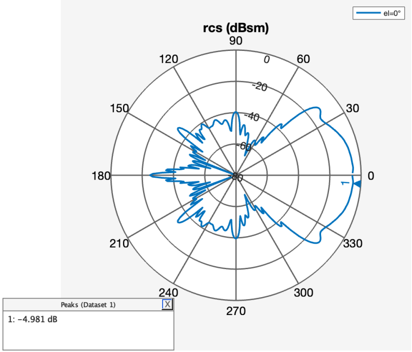

Figure 3.6. 2D RCS of trihedral reflector

Radar cross section (RCS)

- 3D RCS views for both reflectors

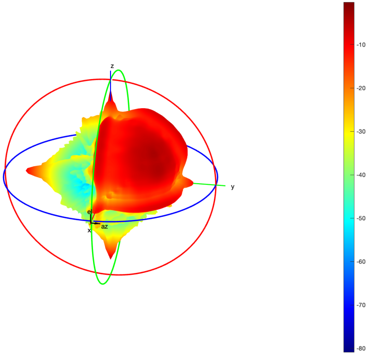

Figure 3.7. 3D RCS of trihedral reflector

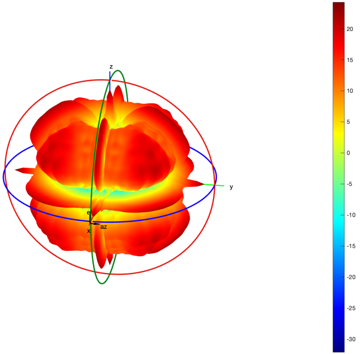

Figure 3.8. 3D RCS of octahedral reflector

Results

- The CFAR plots about the RCS pattern

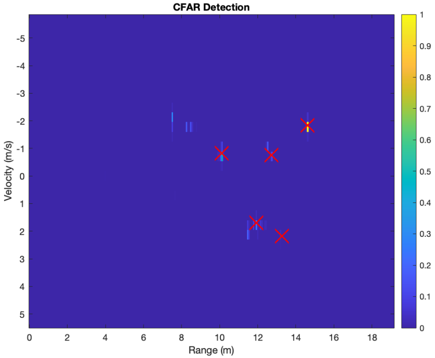

Figure 3.9. With isotropic RCS pattern

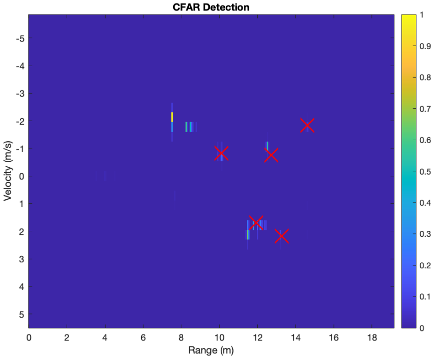

Figure 3.10. With anisotropic RCS pattern

Table of Contents

Trajectory generation

- The trajectory generation for the robot along the wall and furniture

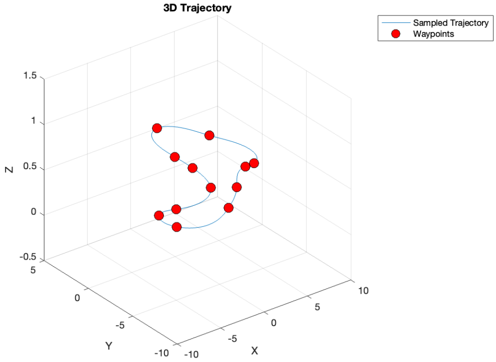

Figure 4.1. The trajectory of the robot

Orientation

- The orientation of the antenna during motion

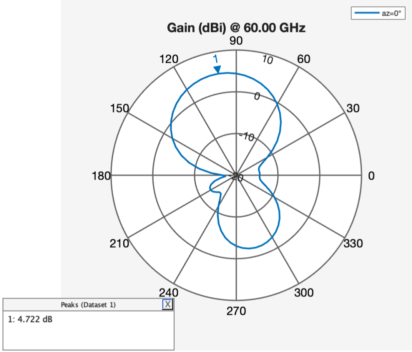

Figure 4.2. Radiation pattern before rotation

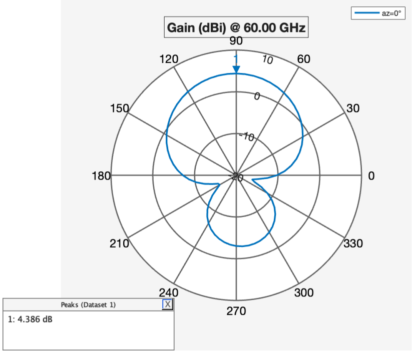

Figure 4.3. Radiation pattern after rotation

Table of Contents

Evaluation

- The CFAR plots difference in units watt (W) and decibel watt (dBW)

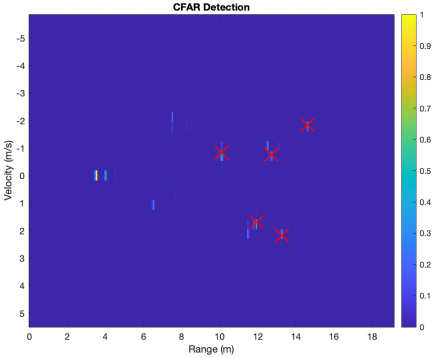

Figure 5.1. CFAR plot in unit W

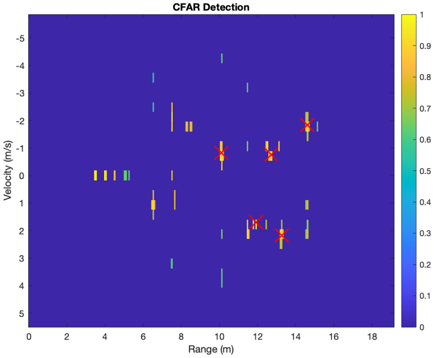

Figure 5.2. CFAR plot in unit dBW

- The CFAR plots with various positions and amount of reflectors in unit W

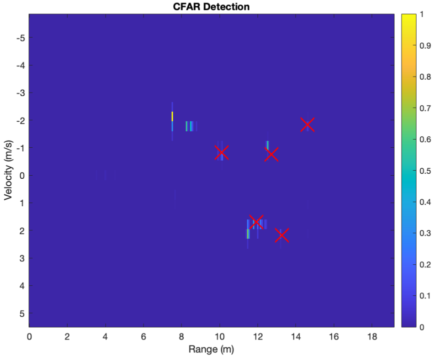

Figure 5.3. CFAR plots with five trihedral corner reflectors

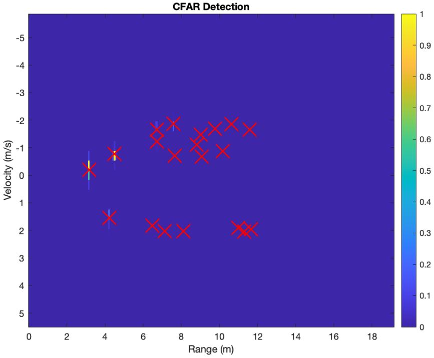

Figure 5.4. CFAR plots with multiple octahedral reflectors

- The meaning of the unit in the case of the multiple reflectors

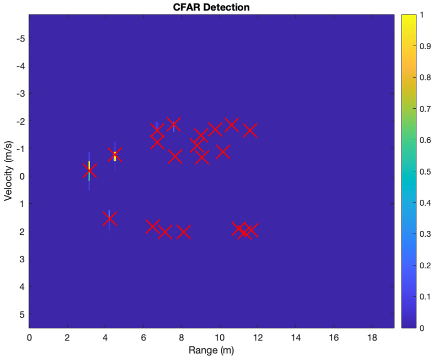

Figure 5.5. CFAR plots in the unit W

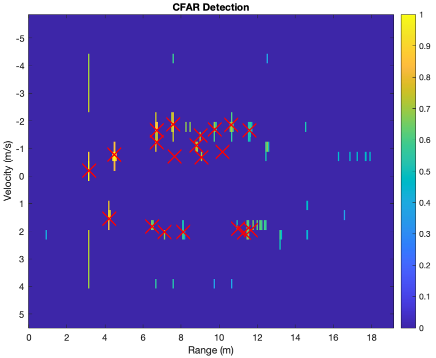

Figure 5.6. CFAR plots in the unit dBW

- The CFAR plots along the trajectory generated in GIF format

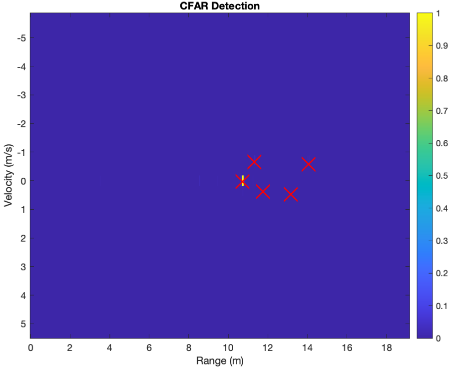

Figure 5.7. CFAR plots along the trajectory

Table of Contents

Summary and outlook

- Summary: The ray tracing channel model works well and meets the goal.
- Outlook:
  - Ray tracing with the surface diffraction
  - Antenna designer
  - RCS pattern simulation without scaling
  - Parallelizable computation of the simulation on GPU
  - Optimization of the number and arrangement of the reflectors
  - Combining with the deep learning for indoor localization system

Reference

[1] Pascal Schlachter et al. *Indoor Positioning based on Active Radar Sensing and Passive Reflectors: Concepts & Initial Results*. 2024. URL: http://arxiv.org/abs/2310.04231.

[2] Stephan Haefner. "Parameter estimation for broadband mm-wave FMCW MIMO radars - a model-based system identification perspectiv". PhD thesis. TU Ilmenau, 2021, pp. 51–56.

[3] *Furniture Free 3D Models Blender - .blend download - Free3D*. URL: https://free3d.com/3d-models/blender-furniture.

[4] K.R. Schaubach, N.J. Davis, and T.S. Rappaport. "A ray tracing method for predicting path loss and delay spread in microcellular environments". In: Denver, CO, USA: IEEE, 1992, pp. 932–935.

[5] M. A. Richards et al., eds. *Principles of modern radar*. SciTech Pub, 2010, pp. 59–66.

[6] Monika Ouza, Michael Ulrich, and Bin Yang. "A simple radar simulation tool for 3D objects based on blender". In: *2017 18th International Radar Symposium (IRS)*. IEEE, 2017, pp. 2–3.

[7] Matthias Kronauge and Hermann Rohling. "New chirp sequence radar waveform". In: *IEEE Transactions on Aerospace and Electronic Systems* 50 (2014), pp. 2870–2877.

Thank you for your attention